Measurement of absolute differential cross sections for the vibrational excitation of molecular nitrogen by electron impact in the $^2\Pi_g$ shape resonance region

Christopher J. Sweeney* and Tong W. Shyn
Space Physics Research Laboratory, University of Michigan, Ann Arbor, Michigan 48109-2143
(Received 7 August 1996; revised manuscript received 30 April 1997)

By means of a crossed-beam technique, we have conducted measurements of absolute differential cross sections for the vibrational excitation of the electronic ground state of N_2 by electron impact. The $^2\Pi_g$ shape resonance region was treated, with the impact energies being those of the resonance's first four elastic scattering peaks—approximately 1.9, 2.1, 2.4, and 2.6 eV. The scattering angles covered were from 12° through 156°, in 12° increments. Absolute integrated-excitation cross sections were computed from the differential cross sections. Our results show the expected strong *D*-wave character, and are compared with the recent results of others, both experimental and theoretical. [S1050-2947(97)06608-0]

PACS number(s): 34.80.Gs

I. INTRODUCTION

Although collision resonances have been of keen interest in nuclear physics for more than half a century now [1], they have only more recently shown their worth in atomic and molecular physics [2,3]. Here they have become particularly valuable for probing the structure of normally vacant electronic orbitals, and are additionally of central importance in the quantum theory of collision processes [4]. A variety of atomic and molecular collision resonances have been discovered in the past two or three decades, and of the electron-molecule resonances in particular, the one arising in the e^--N_2 collision system at impact energies in the vicinity of 2.3 eV has received by far the most attention. This shape resonance, whose symmetry is $^2\Pi_g$, is formed by the addition of a π_g electron to neutral molecular nitrogen in its ground $X^1\Sigma_g^+$ electronic state. The resonance is particularly well known for its role in enhancing the likelihood for nuclear-vibrational excitation of the neutral molecule during collisions with electrons, which is what we shall discuss here.

Besides its importance in atomic and molecular physics, this resonantly enhanced electron collision process has crucial implications in aeronomy, geophysics, and planetary science. In the atmospheres of the Earth and also of several other planets and their moons, the collision cross sections' magnitudes determine in part energy deposition rates, thus affecting atmospheric thermal structure [5–9]. For the Earth, this is particularly relevant with respect to secondary electrons in the *F* region of the ionosphere [10–12]. The e^--N_2 resonance is furthermore of critical technological importance, playing a central role in gas discharge processes such as the one that drives the CO_2-N_2 laser [13,14]. We see that there is thus much justification for the substantial attention this resonance has received over the years in both pure and applied branches of science.

Since the pioneering experiments of Ramsauer and Kollath in the early 1930s there have been numerous measurements of many different aspects of this resonance [15]. Over the years a number of review articles detailing these efforts have appeared, and as a result a good picture of what has happened experimentally up until about a decade ago is now available. (See, e.g., Ref. [16].) We will therefore limit our discussion to only the most recent measurements. These include the treatment of Brunger *et al.*, who determined the cross sections for excitation of the first four vibrational states [17]. They covered the impact energies 2.1, 2.4, and 3.0 eV, and employed the angular range from 10° through 90°. Brennan *et al.* also recently performed vibrational-excitation measurements on N_2 [18]. They obtained differential cross sections for excitation of the first few vibrational levels at 1.5-, 2.1-, 3.0-, and 5.0-eV impact, and covered the scattering angle range from 5° to 130°. Their results compare reasonably well with other experimental results. In some cases, however, they found serious discrepancies among their cross sections and those predicted by theorists. They indicated that these discrepancies could easily have arisen from small errors in energy calibration, as the cross sections are predicted to vary quite wildly with impact energy. The most up-to-date and extensive studies of this resonant scattering process are due to Sun *et al.*, who measured cross sections for elastic scattering and excitation of the first vibrational level, in addition to computing them theoretically [19]. They furthermore established a protocol for comparing the cross sections that is independent of impact energy calibration. Their measurements and predictions agree remarkably well, but unfortunately they did not measure cross sections for excitation of higher vibrational levels, and were limited in their experiments to scattering angles of 130° and lower.

Just as with the experiments, theoretical treatments of this resonance began in the 1930s [20,21]. Plenty of additional theoretical treatments have been conducted since then, and the scientific literature is replete with accounts of them. Again, complete discussions of these are available elsewhere, so we limit our discussion to the most recent ones. (See, e.g., Ref. [22].) For the most part the results of the theoretical calculations were compared with measured total

*Also at Department of Physics, University of Michigan, Ann Arbor, MI 48109-1120, and Comprehensive Studies Program, University of Michigan, Ann Arbor, MI 48109-1003.

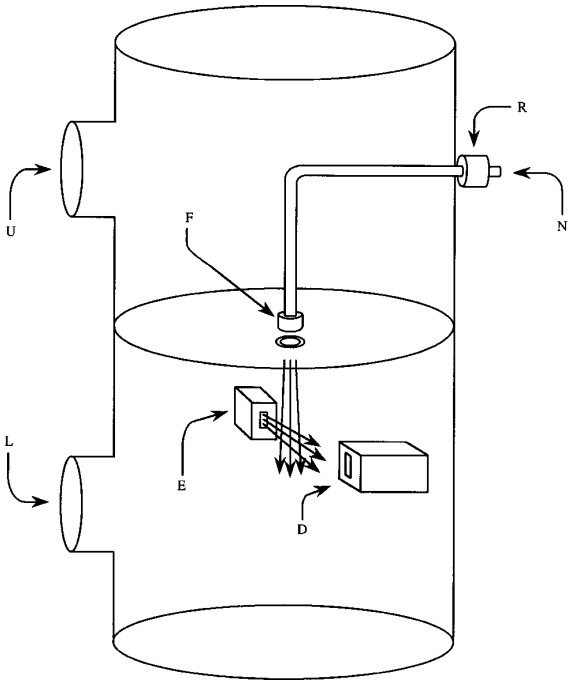

FIG. 1. Schematic overview of the vacuum enclosure along with our apparatus's principal subsystems. E denotes the electron-beam source, D the scattered-electron detector, F the fused-capillary array, and R the flow regulator for the molecular beam. Molecular nitrogen enters at the point labelled N. The entrances to the upper and lower turbomolecular pumps are indicated by U and L, respectively. Portraying the crossed electron and molecular beams are the crossed arrows near the center of the diagram. For simplicity, the Helmholtz coils surrounding the vacuum system are not shown.

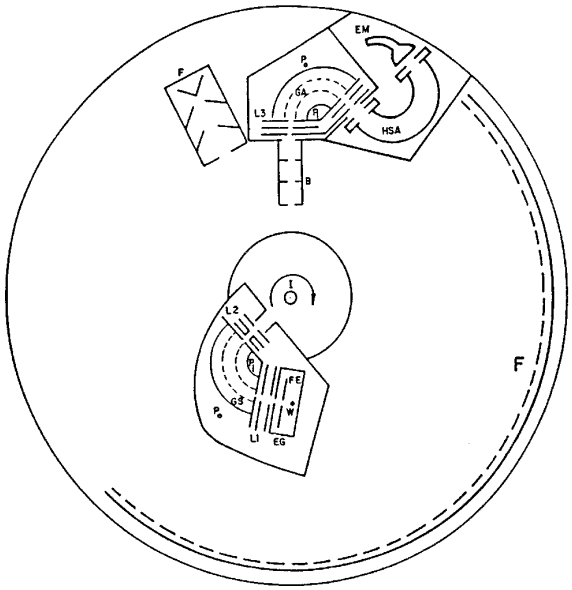

FIG. 2. Schematic overview of the collimated, monoenergetic electron-beam source and scattered-electron detector. In the rotatable electron-beam source located near the center of the diagram, the electron gun is labelled EG, its focusing electrode FE, and its filament W. The two lens systems of the electron-beam source are denoted $L1$ and $L2$. Labelling its energy selector's grids, inner, and outer plates are the symbols GS, P_i, and P_o, respectively. The entire electron-beam source can be rotated about the molecular beam denoted I in the fashion shown by the curved arrow. The molecular beam is directed into the plane of the page. For the scattered-electron detector shown near the top of the diagram, B indicates the entrance baffle, and GA, P_i, and P_o, its cylindrical energy analyzer's grids, inner and outer plates, respectively. $L3$ and $L4$ label the detector's two lens systems, while HSA and EM indicate its hemispherical energy analyzer and Channeltron electron multiplier, respectively. The symbol F is used to denote the two Faraday cups in our apparatus, which are used to monitor the incident electron beam's strength.

cross sections. However, calculations like those of Weatherford and Temkin [12] have emphasized differential cross sections. Their results agree well with the recent experimental results of Brunger *et al.* [17] and Brennan *et al.* [18] with regard to angular shape, but tend to predict magnitudes greater than those determined by these experiments. Weatherford and Temkin emphasized the fact that the cross sections' magnitudes vary extremely rapidly with impact energy in the $^2\Pi_g$ resonance region, and suggested that this was the origin of the discrepancy, as did Sun *et al.*

As a result of the many studies, substantial progress has been made in understanding the nature of this resonance. However, information is still lacking with regard to excitation of higher vibrational levels, especially in the backscattering region. Such data are important as they represent conditions of relatively high momentum transfer, and allow the calculation of integrated cross sections from the differential ones without extensive extrapolation. The dearth of these data is what motivated our research. In this article we present the results of measurements of absolute differential cross sections for excitation of the first few vibrational levels of molecular nitrogen's ground electronic state by electron impact in the $^2\Pi_g$ shape resonance region. Our measurements were performed by a crossed-beam technique, and covered the scattering angle range from 12° to 156°, in 12° increments. The impact energies we employed match those of the first four peaks in the elastic scattering resonance—approximately 1.9, 2.1, 2.4, and 2.6 eV. Absolute integrated vibrational-excitation cross sections were computed from the differential cross sections. Our results show the expected strong D-wave character, and are compared with the recent results of others, both experimental and theoretical.

II. EXPERIMENT

The apparatus we use to conduct our electron-atom and electron-molecule collision experiments is of the crossed-beam type. We shall provide here only a rudimentary account of it, as detailed accounts can be found elsewhere [23–25]. Its key subsystems—the neutral-molecular-beam source, the collimated, monoenergetic electron-beam source, and the scattered-electron detector—along with its typical operating conditions and our experimental procedures, are described in this section.

A. Vacuum system and molecular-beam source

Housing the key subsystems is a vacuum enclosure, as shown schematically in Fig. 1. The enclosure is divided into upper and lower chambers, which are pumped differentially by turbomolecular pumps backed by mechanical rotary

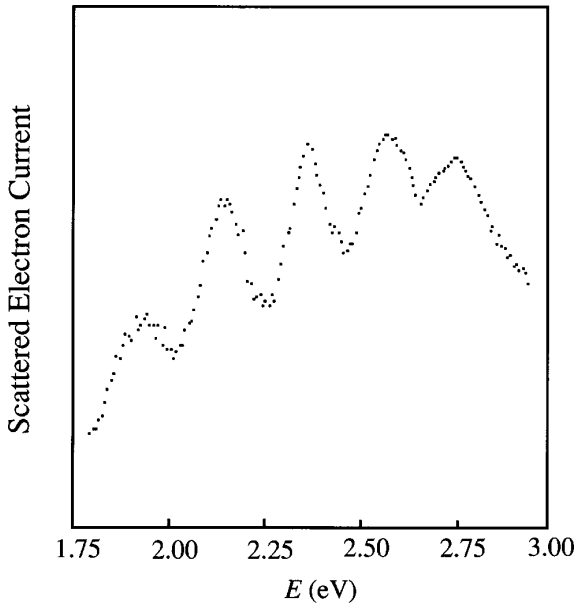

FIG. 3. Typical intensity vs energy spectrum for the elastic scattering of electrons by molecular nitrogen in the $^2\Pi_g$ shape resonance region. The scattering angle was 96°.

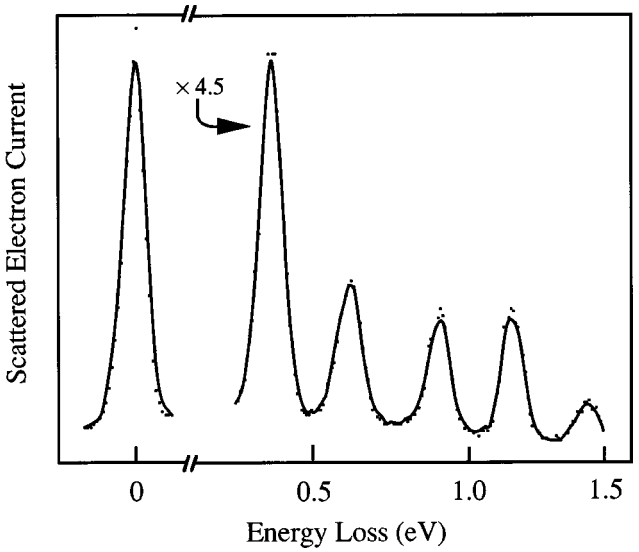

FIG. 4. Typical electron energy-loss spectrum for the vibrational excitation of molecular nitrogen's electronic ground state by electron impact. 2.4 eV was the impact energy, while the scattering angle was 72°. The elastic scattering peak is leftmost, and proceeding to the right are the peaks corresponding to excitation of the first five vibrational levels. Note the change in scale by a factor of 4.5 in the right-hand side of the figure.

pumps. Three mutually perpendicular sets of Helmholtz coils surround the vacuum enclosure and attenuate magnetic fields, including the Earth's, to less than 20 mG in any direction within the interaction region. The proximity of our detector to the interaction region limits the maximum spurious angular deviation imparted to a scattered electron by these fields to less than 2°. This is negligible in comparison to our other experimental sources of uncertainty.

Molecular nitrogen is allowed to flow into the vacuum enclosure from a commercial storage cylinder. Both the flow rate and flow pressure of the N_2 are controlled by a regulator. The tubing that carries the molecular nitrogen to the interaction region enters the upper chamber and terminates at a fused-capillary array located at the junction between the two chambers. The array provides a downwardly directed molecular beam in the lower chamber, where the electron-molecule collisions occur. The molecular beam's angular divergence is no more than $\pm 5°$ full width at half maximum (FWHM).

B. Electron-beam source and scattered-electron detector

Located near the top of the lower chamber are the electron-beam source and scattered-electron detector. They occupy a horizontal plane perpendicular to the axis of the molecular beam, as shown schematically in Fig. 2. The electron-beam source is rotatable continuously from -90 to 160°. It is composed of an electron gun based on a tungsten filament, a 127° cylindrical energy selector, two electron lens systems, and both vertical and horizontal beam deflectors. This subsystem is capable of producing an electron beam of current exceeding 10^{-8} A. The beam's angular divergence profile is very nearly Gaussian in character and has a FWHM no more than $\pm 3°$.

Fixed to the lower chamber's wall is the scattered-electron detector. Comprising this detector are a 127° cylindrical and a hemispherical energy analyzer in tandem, two electron lens systems, and a Channeltron electron multiplier. Such a dual analyzer arrangement provides a signal-to-noise ratio more than 100 times greater than that of our previous single analyzer system [26]. The detector subtends a solid angle of about 5×10^{-4} sr.

Now the net energy resolution profile of our apparatus is the convolution of the energy profile of the electron beam with the response profile of the electron detector. For the present measurements this net profile was very nearly Gaussian in form, and was set to about 80 meV FWHM. Note that while such an energy resolution allows us to see distinct vibrational excitations in our electron energy-loss spectra, it does not allow us to discern individual rotational excitations. All our results are therefore rotationally inelastic.

C. Operating procedures and sample measured spectra

Before any measurements are made, the resonant elastic scattering peak positions are established by measurement of the resonantly enhanced elastic scattering of electrons by molecular nitrogen in the $^2\Pi_g$ region. For all our measurements this was done at a scattering angle of 96°. A typical elastic spectrum resulting from this process is provided in Fig. 3. The four pronounced maxima in the diagram—at approximately 1.9, 2.1, 2.4, and 2.6 eV—represent the energies where the elastic resonant scattering is at its most intense. They were impact energies we subsequently used for our vibrational-excitation experiments, and for convenience we will use these numbers to label the impact energies we employed in the balance of this article. Note, however, that these energies are only approximate. What is important here is that they correspond to the elastic scattering peaks at a specified scattering angle, in accord with the protocol established by Sun *et al.* [19]. The specification of the angle is

TABLE I. Uncertainties (in %) for the present measurements.

Source of uncertainty	E (eV) 1.9	2.1	2.4	2.6
Raw data	±15	±12	±12	±10
Scattered-electron detector efficiency	±10	±10	±10	±10
Elastic cross sections	±14	±14	±14	±14
Total	±23	±21	±21	±20

critical, because as Rohr has shown the energies of the resonant peaks change with angle [27].

The vibrational-excitation measurements were performed slightly differently. Here the energy of the electron beam was fixed, while the energy acceptance window of the detector was swept over the energy-loss region of interest. This process was repeated over the prescribed range of scattering angles and impact energies. The results are energy-loss spectra like that shown in Fig. 4, which is for an impact energy of 2.4 eV and a scattering angle of 72°. Dots denote actual data points, while the solid curve indicates a fit to them. The leftmost peak in the figure represents elastic scattering. Proceeding to the right, the next peaks represent excitation of the nitrogen molecule to its first through fifth excited vibrational levels. Curiously, some of the higher vibrational levels have excitation intensities comparable the lower ones. This effect has been observed before, and ignited much of the interest in the electron-molecular nitrogen collision process.

III. DATA ANALYSIS

To extract collision cross sections from our measured spectra, we employed a process similar to the one we recently used to analyze data for the Schumann-Runge continuum of molecular oxygen [28]. The procedure involved first the correction of our raw spectra for the effects of detection efficiency with respect to energy loss. The resulting corrected spectra were next analyzed using numerical least-squares techniques. Parameters resulting from this analysis were then employed to calculate absolute differential cross sections, and the latter were used to numerically compute absolute integrated cross sections. In this section we cover the details of this entire process, and also indicate the uncertainty present in our results.

A. Correction for detection efficiency

Before any reliable cross sections could be extracted from our spectra, it was essential that these spectra be corrected for the detector's sensitivity to scattered electrons with respect to their energies. To this end, we measured the energy spectra of secondary electrons ejected by electron impact on helium in the region a few eV above the ionization threshold. The yield of secondary electrons in this region is known to be quite nearly constant with respect to impact energy [29–31], so any deviation from constancy in the helium spectra would be a direct manifestation of changing detection efficiency with respect to energy. These spectra were found to vary smoothly with energy, and the detector's efficiency was quantitatively characterized by fitting a third-order polynomial to them by the numerical techniques to be described shortly. Higher-order terms in the polynomial showed themselves to be consistently superfluous and were thus omitted. The polynomial determined in this way was subsequently used to correct our measured molecular nitrogen spectra for detection efficiency.

B. Implementation of least-squares analysis

We employed numerical least-squares techniques to extract physical information from our corrected spectra. For this purpose, we constructed model spectra of the form

$$s(\rho,S_0,\theta,E_i,E_l)=\rho S_0 G(\theta)\sum_{j=0}^{N} f_j(E_i-E_l)I_j(\theta,E_i) + B(E_i-E_l). \quad (1)$$

Here s is the scattered electron signal strength, while ρ is the density of the gaseous target sample in the interaction region, S_0 the signal strength of the incident electron beam, θ the scattering angle, E_i the incident electron beam's energy, and E_l the energy lost by a scattered electron. The factor $G(\theta)$ accounts for differences in scattering volume with respect to angle. For the jth of the N vibrational levels present in a given spectrum, f_j is the normalized Gaussian excitation line shape, while I_j accounts for the excitation intensity associated with this line shape. B represents background contributions, and in our analysis was chosen to be of the quadratic polynomial form

TABLE II. Absolute cross sections for the vibrational excitation of molecular nitrogen's electronic ground state by electron impact at 1.9-eV impact energy. The units for the differential cross sections are 10^{-18} cm^2/sr, while those for the integrated cross sections are 10^{-18} cm^2. Parentheses enclose extrapolated values.

v	θ (deg) 12	24	36	48	60	72	84	96	108	120	132	144	156	168	σ_i
1	66.2	32.5	21.6	15.0	15.5	17.7	17.6	14.7	11.3	10.1	13.5	20.7	31.3	(45.0)	233
2	44.1	27.3	14.6	8.30	7.31	7.46	7.42	5.96	4.19	3.30	3.99	6.61	12.2	(21.5)	112
3	22.0	13.7	5.45	2.62	2.05	1.90	1.89	1.59	1.01	0.734	0.943	1.82	2.80	(4.00)	36.4

TABLE III. Absolute cross sections for the vibrational excitation of molecular nitrogen's electronic ground state by electron impact at 2.1-eV impact energy. The units for the differential cross sections are 10^{-18} cm^2/sr, while those for the integrated cross sections are 10^{-18} cm^2. Parentheses enclose extrapolated values.

	θ (deg)														
	12	24	36	48	60	72	84	96	108	120	132	144	156	168	σ_i
v															
1	71.0	40.3	21.4	15.6	12.4	16.1	19.3	16.0	11.2	10.5	13.1	16.5	30.0	(46.0)	234
2	21.3	15.2	7.65	6.47	6.40	7.66	9.72	9.80	7.69	7.92	11.0	13.2	20.1	(35.0)	129
3	16.0	9.94	8.48	7.80	7.39	8.32	9.35	8.95	7.60	6.37	7.65	9.93	15.0	(20.0)	112
4	13.0	9.96	6.45	4.79	3.74	3.62	3.94	3.68	3.08	4.17	6.87	10.1	14.8	(18.0)	73.3

$$B(E_i-E_l)=\sum_{j'=0}^{2} a_{j'}(E_i-E_l)^{j'}, \tag{2}$$

where the set of $a_{j'}$ are free parameters. Higher-order terms in this polynomial proved themselves superfluous, and were thus omitted.

The model spectra were fit to the corrected spectra via numerical least-squares analysis. During this process, the factors ρ, S_0, and $G(\theta)$ were dispensed with, since they cancel out in a separate normalization procedure, which we shall discuss shortly. (Such factors are already accounted for in the elastic cross sections used for normalization; see, e.g., Ref. [23] for a complete discussion of their determination and values.) The algorithm we used for the least-squares analysis was the nonlinear Levenberg-Marquardt steepest-descents method [32]. While other, more sophisticated least-squares fitting algorithms, such as simulated-annealing [33,34] and neural-network [35] approaches are available, such sophistication was not necessary to model the well resolved excitation peaks present in our molecular nitrogen data. Source code for the fitting program was written in double precision arithmetic in the FORTRAN90 computer language. The program was run on the same computer we used to accumulate and store data. The program's output was the relative intensities of both the elastic and vibrational-excitation line shapes and also their FWHMs.

C. Determination of absolute cross sections

With the intensities and FWHMs of the line shapes in hand, we calculated absolute differential cross sections. To do this, we exploited the fact that cross sections scale as the areas under the excitation line shapes. Recalling that these line shapes were Gaussian, and that the area under a Gaussian is proportional to the product of its maximum height and its FWHM, we were able to relate inelastic and elastic cross sections as

$$\left(\frac{d\sigma}{d\Omega}\right)_{\text{inel}}=\frac{I_{\text{inel}}\Delta_{\text{inel}}}{I_{\text{elas}}\Delta_{\text{elas}}}\left(\frac{d\sigma}{d\Omega}\right)_{\text{elas}}, \tag{3}$$

where the symbols I and Δ correspond to the maximum magnitude and FWHM, respectively. (Note that in the present case the FWHMs are essentially equal and thus effectively cancel.) Absolute values for the differential cross sections were generated from this equation and the absolute elastic differential cross sections measured previously by one of us and a collaborator [36].

Absolute integrated-excitation cross sections, denoted σ_i, were calculated from the absolute-differential cross sections via the trapezoid rule. This required that we extrapolate our results to both 0° and 180°, which we did in a semi-exponential manner. Due to the smallness of the factor $\sin\theta$ in the formula

$$\sigma_i=\int d\varphi\, d\theta \sin\theta\left(\frac{d\sigma}{d\Omega}\right), \tag{4}$$

at these angles, negligible uncertainty was introduced into our results.

D. Propagation of uncertainty

The various sources of uncertainty in our measurements include the raw data (statistical uncertainty), the detector ef-

TABLE IV. Absolute cross sections for the vibrational excitation of molecular nitrogen's electronic ground state by electron impact at 2.4-eV impact energy. The units for the differential cross sections are 10^{-18} cm^2/sr, while those for the integrated cross sections are 10^{-18} cm^2. Parentheses enclose extrapolated values.

	θ (deg)														
	12	24	36	48	60	72	84	96	108	120	132	144	156	168	σ_i
v															
1	53.4	27.7	16.6	11.9	12.5	13.8	14.3	14.0	12.6	14.1	19.1	21.0	32.0	(48.0)	220
2	26.7	20.2	12.5	10.5	11.8	12.9	12.6	11.1	8.53	7.36	8.84	9.61	12.5	(17.0)	145
3	17.9	10.2	6.25	4.02	3.42	3.14	2.84	2.57	2.17	2.56	3.47	5.21	6.30	(9.00)	52.9
4	6.73	3.74	2.31	2.14	2.56	3.15	3.70	4.11	3.80	3.43	3.37	4.01	5.01	(6.20)	44.2

TABLE V. Absolute cross sections for the vibrational excitation of molecular nitrogen's electronic ground state by electron impact at 2.6-eV impact energy. The units for the differential cross sections are 10^{-18} cm^2/sr, while those for the integrated cross sections are 10^{-18} cm^2. Parentheses enclose extrapolated values.

	θ (deg)														
v	12	24	36	48	60	72	84	96	108	120	132	144	156	168	σ_i
1	(40.0)	25.5	17.6	13.2	13.7	14.4	15.3	13.9	13.4	13.3	20.8	35.0	43.6	(59.0)	242
2	(14.0)	12.7	9.92	8.06	8.39	8.64	8.50	7.26	6.43	6.22	7.20	12.2	19.9	(27.0)	117
3	(7.00)	5.02	3.08	2.48	2.78	3.11	3.59	3.56	3.07	2.68	3.18	3.46	4.50	(5.80)	42.5
4	(4.70)	3.53	3.09	2.59	3.07	3.65	4.06	3.80	3.87	2.77	3.10	3.44	4.44	(5.50)	44.0

ficiency, and the elastic cross sections used for normalization. As these sources are independent of each other, their values were added in quadrature to provide the net uncertainty. Values for these sources of uncertainty, along with the net uncertainties at each impact energy, are provided in Table I.

IV. DISCUSSION OF RESULTS

In its ground $X^1\Pi_g^+$ electronic state, the neutral nitrogen molecule has the electronic configuration [37]

$$(\sigma_g 1s)^2(\sigma_u 1s)^2(\sigma_g 2s)^2(\sigma_u 2s)^2(\pi_u 2p)^4(\sigma_g 2p)^2.$$

During an electron collision, the $^2\Pi_g$ resonance (which is the ground electronic state of the negative molecular nitrogen ion) is formed if the impinging electron falls into the energetically lowest vacant orbital, which has π_g $2p$ symmetry in the separated-atom scheme, and $3d$ π_g symmetry in the united-atom scheme. This resonance has a lifetime of approximately the period of one nuclear vibration, and may decay by autoionization, thus completing the collision process. The ejected electron needs to penetrate an $l=2$ angular momentum barrier to escape the N_2 core during autoionization, so we expect the electron's angular distribution to be D wave in character [3]. The energy profile of the resonance exhibits multiple maxima, which arise from interference between the outgoing and reflected nuclear quantum states during the collision; these peaks therefore correspond to the nuclear-vibrational levels of the negative molecular nitrogen ion only approximately [38]. Our measurements were performed at impact energies where resonant elastic scattering into 96° exhibits its peaks—at approximately 1.9, 2.1, 2.4, and 2.6 eV.

As we see from the absolute numerical values for the cross sections presented in Tables II, III, IV, and V, and their graphical depictions in Figs. 5 and 6, strong D-wave character is in fact present. Figure 5 displays the differential cross sections for excitation of the first three vibrational levels of N_2 at 1.9-eV impact. Here the forward scattering is a little stronger than the backward scattering, indicating the substantial presence of both direct and resonant components to the scattering process. This is especially noticeable for the excitation of the third vibrational level. For the two local minima present in the angular distributions, the lower one moves from about 50° to about 75° as the vibrational quantum number increases, while the upper one remains at a nearly constant location of about 120°. The magnitudes of the cross sections follow the usual pattern, with the $v=1$ results being the largest, and the $v=3$ results being the smallest.

Displayed in Fig. 6 are the differential cross sections for the lowest four vibrational levels at 2.4-eV impact. The two

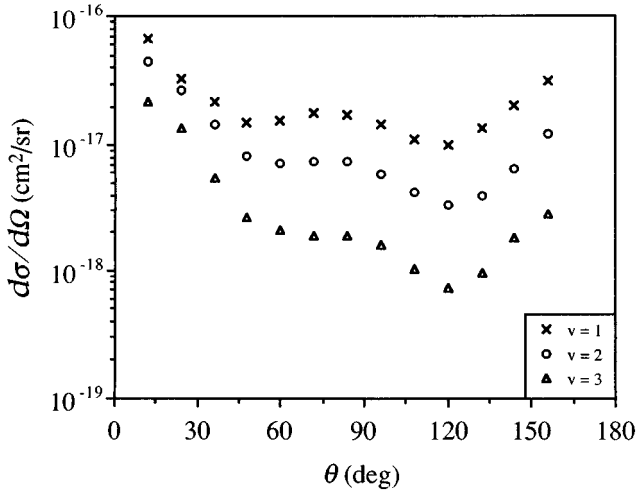

FIG. 5. Absolute differential cross sections for the vibrational excitation of molecular nitrogen by electron impact at 1.9-eV impact energy.

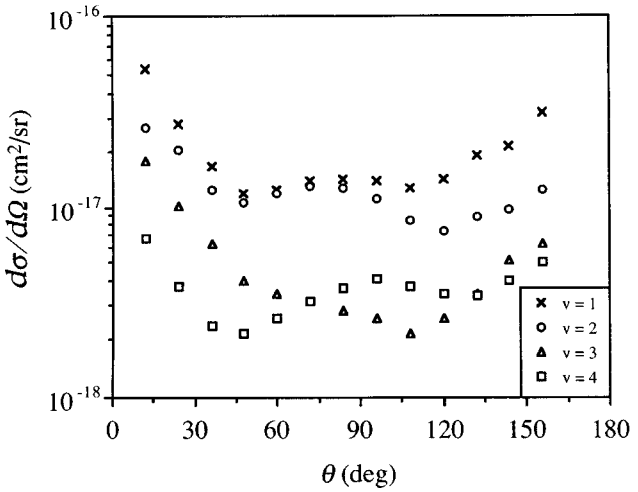

FIG. 6. Absolute differential cross sections for the vibrational excitation of molecular nitrogen by electron impact at 2.4-eV impact energy.

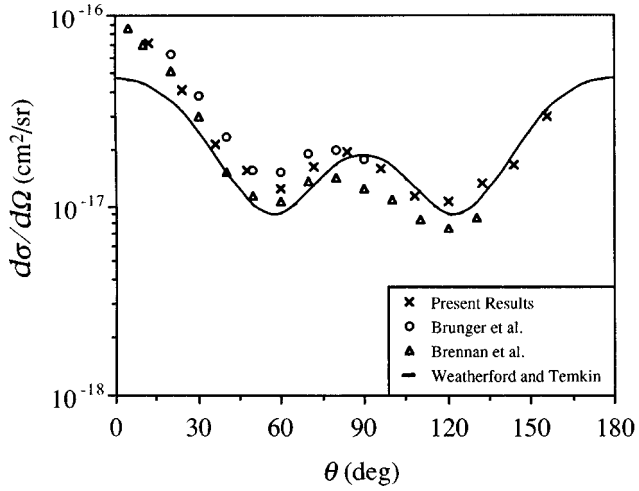

FIG. 7. Comparison of absolute differential cross sections for excitation of the first vibrational level of molecular nitrogen by electron impact at 2.1-eV impact energy.

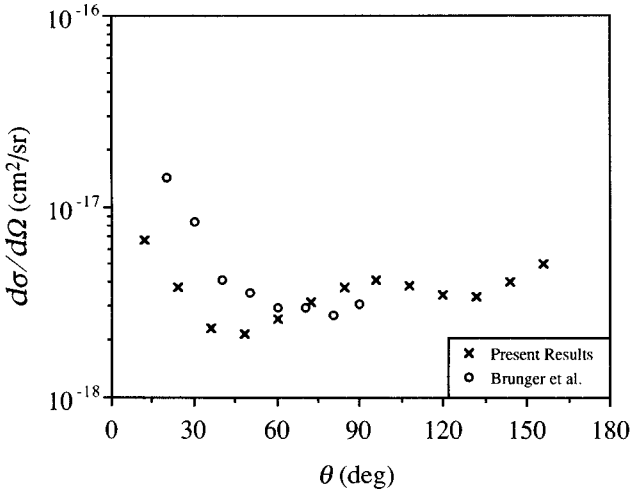

FIG. 9. Comparison of absolute differential cross sections for excitation of the fourth vibrational level of molecular nitrogen by electron impact at 2.4-eV impact energy.

relative minima in this case hover around 45° and 100° as the vibrational quantum number increases, with the lower minimum nearly disappearing in the presence of the strong forward scattering for excitation of the third vibrational level. Here the cross sections for excitation of the first and second vibrational levels are of almost equal magnitude at middle angles, while the cross sections for excitation of the fourth vibrational level exceed those for excitation of the third at high angles.

We compare our 2.1-eV impact differential cross sections for excitation of the first vibrational level with those measured by Brunger *et al.* [17] and Brennan *et al.* [18], and with those calculated by Weatherford and Temkin [12] in Fig. 7. All the cross sections compare resonably well. Our results are generally intermediate in magnitude relative to the other experimental ones. Weatherford and Temkin's calculated cross sections lie below ours at low and middle angles, but are in good agreement with ours at high angles. This suggests that the calculated direct component is less than the measured one. Differences among the cross sections may be attributable chiefly to small differences in impact energy—none of the cross sections were determined at exactly 2.1-eV impact, and ours were the only ones measured in accordance with the protocol of Sun *et al.* With much of the available data and calculations not following this protocol both here and in several of the following paragraphs, this sort of comparison was unfortunately the only one possible.

Our $v=1$ excitation differential excitation cross sections are compared with the very recent results of Sun *et al.* in Fig. 8. The two results are generally of the same order of magnitude, but discrepancies clearly exist. While both results show strong D-wave character, this character is somewhat more pronounced in the cross sections of Sun *et al.* Theirs is much closer to a pure D wave, showing more substantial minima in the neighborhoods of 60° and 120°. One would also be led to strongly suspect that our cross sections represent the case of substantially higher backscattering, though this cannot be inferred for sure, as their cross-section measurements were not performed at angles any higher than 130°. Such descrep-

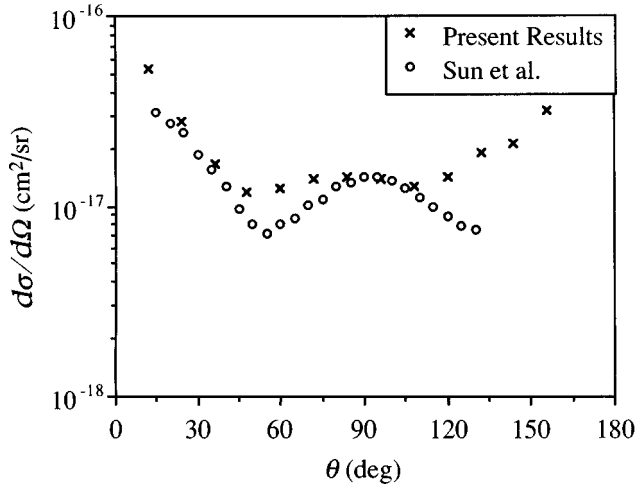

FIG. 8. Comparison of absolute differential cross sections for excitation of the first vibrational level of molecular nitrogen by electron impact at 2.4-eV impact energy.

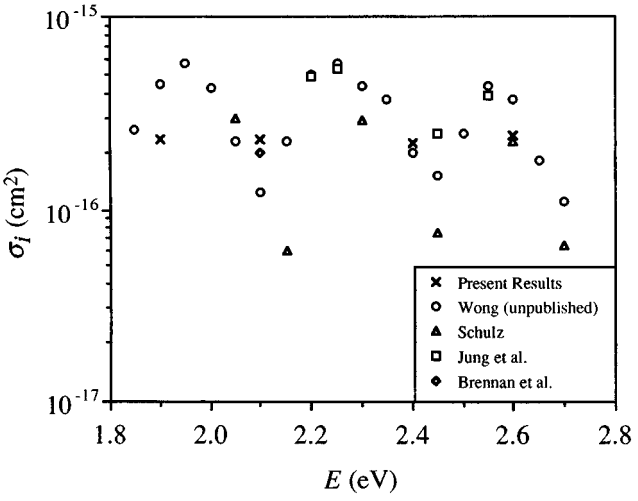

FIG. 10. Comparison of absolute integrated cross sections for excitation of the first vibrational level of molecular nitrogen by electron impact.

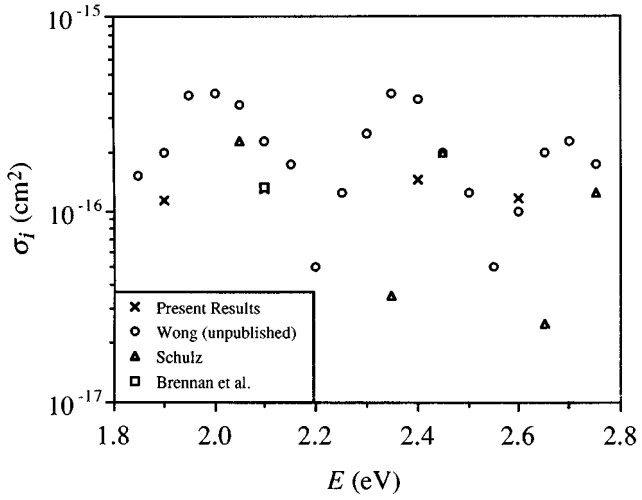

FIG. 11. Comparison of absolute integrated cross sections for excitation of the second vibrational level of molecular nitrogen by electron impact.

ancies are likely to stem from the combination of two sources. First, the elastic cross sections used for normalization purposes were not the same. Secondly, the scattering angles used for determination of the elastic resonance positions were not the same. We used 96°, while they used 60°. As we indicated before, this is critical as Rohr has shown that these positions vary with angle.

In Fig. 9, we compare our 2.4-eV impact cross sections for excitation of the fourth vibrational level with those of Brunger *et al.* [17]. Their cross sections have a much stronger forward component than ours, and possess what may be a local minimum at about 80°, while our cross sections have local minima around 45° and 120°.

Figure 10 shows our absolute integrated cross sections for excitation of the first vibrational level along with the results of Wong (see the article by Dubé and Herzenberg for further discussion of Wong's results [39]), of Schulz [14], of Jung *et al.* [40], and of Brennan *et al.* [18]. Our result is lower than Wong's at 1.9-eV impact, but agrees well with that of Brennan *et al.* at 2.1-eV impact. We are in accord with Wong at 2.4-eV impact, and with Schulz at 2.6-eV impact. Our cross section is lower than Wong's at this latter impact energy, however.

In Fig. 11 we compare our integrated cross sections for excitation of the second vibrational level with those of Wong, of Schulz, and of Brennan *et al.* There is striking agreement between us and the latter researchers at 2.1-eV impact, while our cross section at 2.6-eV impact compares well with Wong's at this energy. At other energies, though, agreement is not as good. As Brennan *et al.* and Weatherford and Temkin have indicated, these discrepancies may well be due to slight differences in impact energy.

V. CONCLUSION

Using a crossed-beam technique, we have measured absolute differential cross sections for the vibrational excitation of molecular nitrogen by electron impact in the $^2\Pi_g$ shape resonance region. The scattering angles covered were from 12° through 156° in 12° increments, while the impact energies used were those of the first four elastic scattering resonant peaks—approximately 1.9, 2.1, 2.4, and 2.6 eV. The expected dominant D-wave character was observed in the absolute differential cross sections. Our results extend the experimentally obtained cross sections to higher-lying vibrational states and into the backward scattering region.

ACKNOWLEDGMENTS

We are grateful for support for this research provided by the University of Michigan's Office of the Vice President for Research, by the Michigan Space Grant Consortium, and by the National Science Foundation under Grant No. ATM-9415678. We are further indebted to Professor J. W. Rasul, Dr. A. Temkin, and Professor J. C. Zorn for valuable conversations regarding atomic and molecular collision resonances. Professor T. L. Killeen is also acknowledged for providing important insight into the role of e^--N_2 scattering in atmospheric processes.

[1] J. M. Blatt and V. F. Weisskopf, *Theoretical Nuclear Physics* (John Wiley & Sons, Inc., New York, 1952).
[2] G. J. Schulz, Rev. Mod. Phys. **45**, 378 (1973).
[3] G. J. Schulz, Rev. Mod. Phys. **45**, 423 (1973).
[4] L. D. Landau and E. M. Lifshitz, *Quantum Mechanics (Non-relativistic Theory)*, 3rd English ed. (Pergamon Press, Oxford, 1977).
[5] P. B. Hays and W. E. Sharp, J. Geophys. Res. **78**, 1153 (1973).
[6] R. W. Schunk and P. B. Hays, Geophys. Res. Lett. **2**, 239 (1975).
[7] J. P. Doering, W. K. Peterson, C. O. Bostrom, and T. A. Potemra, Geophys. Res. Lett. **3**, 129 (1976).
[8] W. J. McMahon and L. Heurox, J. Geophys. Res. **83**, 1390 (1978).
[9] C. J. Gillan, J. Tennyson, B. M. McLaughlin, and P. G. Burke, J. Phys. B **29**, 1531 (1996).
[10] A. V. Phelps, in *Electron-Molecule Scattering*, edited by S. C. Brown (John Wiley & Sons, Inc., New York, 1979).
[11] A. V. Phelps and L. C. Pitchford, Phys. Rev. A **31**, 2932 (1985).
[12] C. A. Weatherford and A. Temkin, Phys. Rev. A **49**, 2580 (1994).
[13] D. C. Tyte, in *Advances in Quantum Electronics*, edited by D. N. Goodwin (Academic Press, London, 1970).
[14] G. J. Schulz, in *Principles of Laser Plasmas*, edited by B. Befeki (John Wiley & Sons, Inc., New York, 1976).
[15] C. Ramsauer and R. Kollath, Ann. Phys. (Leipzig) **10**, 143 (1931).
[16] Y. Itikawa, M. Hayashi, A. Ichimura, K. Ondo, K. Sakimoto, K. Takayanagi, M. Nakamura, H. Nishimura, and T. Takayanagi, J. Phys. Chem. Ref. Data **15**, 985 (1986).
[17] M. J. Brunger, P. J. O. Teubner, A. M. Weigold, and S. J.

Buckman, J. Phys. B **22**, 1443 (1989).
[18] M. J. Brennan, D. T. Alle, P. Euripides, S. J. Buckman, and M. J. Brunger, J. Phys. B **25**, 2669 (1992).
[19] W. Sun, M. A. Morrison, W. A. Isaacs, W. K. Trail, D. T. Alle, R. J. Gulley, M. J. Brennan, and S. J. Buckman, Phys. Rev. A **52**, 1229 (1995).
[20] H. C. Stier, Z. Phys. **76**, 439 (1932).
[21] J. B. Fisk, Phys. Rev. **49**, 167 (1936).
[22] N. F. Lane, Rev. Mod. Phys. **52**, 29 (1980).
[23] T. W. Shyn, R. S. Stolarski, and G. R. Carignan, Phys. Rev. A **6**, 1002 (1972).
[24] T. W. Shyn, C. J. Sweeney, and A. Grafe, Phys. Rev. A **49**, 3680 (1994).
[25] C. J. Sweeney and T. W. Shyn, Phys. Rev. A **53**, 1576 (1996).
[26] T. W. Shyn, Phys. Rev. A **27**, 2388 (1983).
[27] K. Rohr, J. Phys. B **11**, 2215 (1977).
[28] T. W. Shyn, C. J. Sweeney, A. Grafe, and W. E. Sharp, Phys. Rev. A **50**, 4794 (1994).
[29] S. Cvejanović and F. H. Read, J. Phys. B **7**, 1841 (1974).
[30] D. Spence, Phys. Rev. A **11**, 1539 (1975).
[31] F. Pichou, A. Huetz, G. Joyez, M. Landau, and J. Mazeau, J. Phys. B **9**, 933 (1976).
[32] W. H. Press, B. P. Flannery, S. A. Teukolsky, and W. T. Vetterling, *Numerical Recipes*, 2nd ed. (Cambridge Univ. Press, Cambridge, 1992).
[33] S. Kirkpatrick, C. D. Gelatt, Jr., and P. Vecchi, Science **220**, 671 (1983).
[34] W. H. Press and S. A. Teukolsky, Comput. Phys. **5**, 426 (1991).
[35] W. L. Morgan, IEEE Trans. Plasma Sci. **19**, 250 (1991).
[36] T. W. Shyn and G. R. Carignan, Phys. Rev. A **22**, 923 (1980).
[37] G. Herzberg, *Molecular Spectra and Molecular Structure I. Spectra of Diatomic Molecules*, 2nd ed. (D. van Nostrand Co., Inc., Princeton, NJ, 1950).
[38] D. T. Birtwhistle and A. Herzenberg, J. Phys. B **4**, 53 (1971).
[39] L. Dubé and A. Herzenberg, Phys. Rev. A **20**, 194 (1979).
[40] K. Jung, T. Antoni, R. Müller, K.-H. Kochem, and H. Ehrhardt, J. Phys. B **15**, 3535 (1982).